Nucleosome positioning and gene regulation of the *SGLT2* gene in the renal proximal tubular

epithelial cells

Hiroaki Takesue, Takeshi Hirota, Mami Tachimura, Ayane Tokashiki, Ichiro Ieiri

Department of Clinical Pharmacokinetics, Graduate School of Pharmaceutical Sciences, Kyushu

University

MOL#111807

Running Title: Nucleosome positioning and gene regulation of the *SGLT2* gene

Corresponding author:

Ichiro Ieiri, PhD, Department of Clinical Pharmacokinetics, Graduate School of Pharmaceutical Sciences,

Kyushu University

Address: 3-1-1 Maidashi, Higashi-ku, Fukuoka, 812-8582, Japan

Phone: +81-92-642-6656; Fax: +81-92-642-6660; E-mail: ieiri-ttr@umin.ac.jp

Number of text pages: 35

Number of tables: 0

Number of figures: 8

Number of references: 58

Number of words in the Abstract: 230

Number of words in the Introduction: 493

Number of words in the Discussion: 1354

Abbreviations

5'-FR, 5'-flanking region; AcH3, acetylated histone H3; ChIP, chromatin immunoprecipitation; DMSO,

dimethyl sulfoxide; HNF1α, hepatocyte nuclear factor 1 alpha; NOMe-Seq, nucleosome occupancy and

methylome sequencing; NuSA, nucleosome-scanning assay; PTEC, proximal tubule epithelial cell; SGLT2,

sodium-glucose co-transporter 2; TSA, trichostatin A; TSS, transcription start site

MOL#111807

Abstract

Filtered glucose is mostly reabsorbed by sodium-glucose co-transporter 2 (SGLT2) in the proximal tubules. SGLT2 is predominantly expressed in the human kidney. However, the regulatory mechanisms for *SGLT2* gene expression in the human kidney remain unclear. We herein elucidated the transcriptional regulatory mechanisms for the *SGLT2* gene by nucleosome occupancy in the *SGLT2* promoter region. Expressions of SGLT2 mRNA and protein were markedly weaker in human kidney-derived HK-2 cells than the human kidney. The nucleosome occupancy level in the *SGLT2* promoter region was low in the kidney, but high in HK-2 cells. A treatment with a histone deacetylase inhibitor trichostatin A (TSA) decreased nucleosome occupancy in the promoter region, and increased *SGLT2* expression levels in HK-2 cells. The up-regulation of *SGLT2* expression by histone acetylation was accompanied by a higher binding frequency of hepatocyte nuclear factor 1 alpha (HNF1α), a transcriptional modulator of *SGLT2* in the human kidney, to the promoter region. The transfection of an HNF1α expression plasmid into HK-2 cells resulted in the up-regulation of SGLT2 mRNA expression in the presence of TSA, but not in the treatment of dimethyl sulfoxide as a control. Nucleosome occupancy in the promoter region was markedly higher in the liver and small intestine than the kidney. Our results indicate that tissue-specific nucleosome occupancy plays an important role in the regulation of *SGLT2* gene expression via HNF1α binding at the *SGLT2* promoter region.

Introduction

The kidney plays an important role in the reabsorption of glucose from the glomerular filtrate.

Approximately ~180 g of glucose is typically filtered by the kidneys each day and reabsorbed in proximal

tubule epithelial cells (PTECs) by sodium-glucose co-transporters (SGLTs) (Wright, 2001; Chen *et al.*,

2010; Gerich, 2010; López *et al.*, 2010). In the S1 and S2 segments of the proximal tubule, approximately

90% of filtered glucose is reabsorbed through SGLT2 (Gerich, 2010). Previous studies demonstrated that a

deficiency in SGLT2 expression decreased blood glucose levels. The knockout of *Sglt2* in diabetic mice

reduced blood glucose levels and prevented glomerular hyperfiltration (Vallon *et al.*, 2013). Therefore, the

inhibition of SGLT2 activity in the kidney is regarded as an effective strategy for glycemic control in

diabetic patients. Selective SGLT2 inhibitors have been developed as a new class of oral medication for the

treatment of type 2 diabetes mellitus. These drugs reduce glucose reabsorption by SGLT2 in the proximal

tubules, thereby increasing urinary glucose excretion and lowering plasma glucose levels (Jabbour and

Goldstein, 2008; Boldys and Okopien, 2009; Misra, 2013).

Previous studies focused on the regulation of *SGLT2* expression by transcription factors.

Hepatocyte nuclear factor (HNF) 1α, which has been characterized as a modulator of *SGLT2* expression,

was shown to directly bind to the *SGLT2* 5'-flanking region (5'-FR) and control *SGLT2* gene expression

(Pontoglio *et al.*, 2000; Freitas *et al.*, 2008; Zhao *et al.*, 2016). Additionally, HNF4α and SP1 have been

reported to play an important role in *SGLT2* expression (Kothinti *et al.*, 2010; Bonner *et al.*, 2015).

Although these transcription factors are expressed in various tissues such as the liver and intestines, *SGLT2*

is not. Therefore, another mechanism for the regulation of *SGLT2* expression appears to contribute to tissue-

specific gene expression. The nucleosome is a basic unit of chromatin and consists of approximately 147

bp of DNA wrapped around histones. Nucleosome occupancy plays an important role in the epigenetic

regulation of gene expression by inhibiting the initiation of transcription at gene promoters (Lorch *et al.*,

1987; Workman, 2006). Previous studies demonstrated that nucleosomes control tissue-specific

transcription factor binding to gene promoters, and, thus, contribute to tissue-specific gene expression

(Hoffman *et al.*, 2010; Hu *et al.*, 2011; Tsui *et al.*, 2011; Yang *et al.*, 2013; Zhang *et al.*, 2015). However,

the relationship between nucleosome occupancy and tissue-specific *SGLT2* expression remains unknown.

Therefore, a clearer understanding of nucleosome occupancy at the *SGLT2* promoter may provide

significant insights into transcriptional regulatory mechanisms for the *SGLT2* gene in the human kidney.

In the present study, we focused on the transcriptional regulation of the *SGLT2* gene by

nucleosome occupancy in *SGLT2* 5'-FR in the human kidney. We demonstrated that decreasing nucleosome

occupancy in the *SGLT2* promoter plays a critical role in the up-regulation of *SGLT2* expression. We also

revealed that HNF1α binds to the *SGLT2* promoter in the human kidney, and the activation of *SGLT2*

transcription by HNF1α requires low nucleosome occupancy through histone acetylation in the *SGLT2*

promoter.

Materials and Methods

Human Tissue

A human kidney cortex and small intestine obtained from surgical specimens were purchased

from Integrated Laboratory Services-Biotech (Chestertown, MD). A human liver sample was obtained from

a Caucasian donor at the National Disease Research Interchange (Philadelphia, PA). All assays using human

tissue samples were performed by three independent experiments (n = 3). The use of human tissues was

approved by the Kyushu University Institutional Review Board for Human Genome/Gene Research

(Fukuoka, Japan).

Cell culture

HK-2 cells were obtained from the American Type Culture Collection (Manassas, VA). Cells

were cultured in DMEM/F12 medium (Thermo Fisher Scientific, Waltham, MA) supplemented with 10%

fetal bovine serum at 37°C in an incubator with 5% CO_2.

Construction of SGLT2 reporter plasmids

The DNA fragment of *SGLT2* 5'-FR (-3185/+18) was amplified by a polymerase chain reaction

(PCR) using primers (described as -3185 and +18 in Supplemental Table 1) and human genomic DNA as a

template. The pGL4.10 vector (Promega, Madison, WI) was digested by KpnI and HindIII restriction

enzymes, and then ligated with the PCR product using the In-Fusion® HD Cloning kit (TaKaRa, Shiga,

Japan). Deletion constructs [-2320/+18, -1587/+18, -485/+18, -154/+18, -44/+18, and del-(-51/-37)] were

generated by In-Fusion cloning or the QuikChange II site-directed mutagenesis method (Supplemental

Table 1) using the -3185/+18 construct as a template. The sequences of these plasmids were confirmed by

direct sequencing using primers (Supplemental Table 2) described previously (Nishimura *et al.*, 2014).

6

MOL#111807

Construction of an HNF1α expression plasmid

The coding region of HNF1α was amplified by PCR using cDNA synthesized from the human

kidney and primers (Supplemental Table 3). The pcDNA3.1(+) vector (Invitrogen, Carlsbad, CA) was

digested by EcoRI and EcoRV restriction enzymes, and then ligated with the PCR product using the In-

Fusion® HD Cloning kit. The sequence of the plasmid was confirmed by directed sequencing using primers

(Supplemental Table 3).

Luciferase assay

HK-2 cells were seeded on 24-well culture plates at 0.2×10^5 cells/well and incubated for 24

hours. A series of reporter constructs [equimolar amounts of the empty pGL4.10 plasmid (250 ng)], 500 ng

of the HNF1α expression plasmid or the empty pcDNA3.1(+) plasmid, and 25 ng of the internal standard

pGL4.70 (Promega) were transfected into HK-2 cells using FuGENE® HD Transfection Reagent (Promega)

according to the manufacturer's instructions. After 48 hours, luciferase activities were measured using the

Dual-Luciferase® Reporter Assay System (Promega) and a TD-20/20 Luminometer (Promega).

Transcriptional activities were expressed as the ratio of *Firefly* luciferase to *Renilla* luciferase activity.

RNA interference

The transfection mix was prepared in Opti-MEM (Invitrogen) with HNF1α siRNA (siHNF1α;

Sigma-Aldrich, St. Louis, MO) or control siRNA (MISSION siRNA Universal Negative Control; SIC-001;

Sigma-Aldrich) and Lipofectamine RNAiMAX (Invitrogen) according to the manufacturer's directions.

7

The final concentrations of siRNA and lipofectamine added to the cells were 20 nM and 2 µL/ml, respectively. HK-2 cells were cultured in the presence of the transfection mixture for 24 hours, and cells were treated with dimethyl sulfoxide (DMSO) or 1.0 µM trichostatin A (TSA; Wako, Osaka, Japan) for 24 hours. siHNF1α sequences were: 5'-CAGUGAGACUGCAGAAGUAtt-3' (sense sequence) and 5'-TACTTCTGCAGTCTCACTGtt-3' (antisense sequence).

Total RNA isolation and capture of nascent RNAs

HK-2 cells were seeded on a 6-well plate at 1.5×10^5 cells/well and incubated for 24 hours, and cells were then transfected with 500 ng of an HNF1α expression plasmid or pcDNA3.1(+) plasmid using the FuGENE® HD Transfection Reagent (Promega). After 48 hours, cells were treated with DMSO or 1.0 µM TSA, together with 0.2 mM 5-ethynyl uridine (EU) for 24 hours. Total RNA was isolated from the human kidney and HK-2 cells using ISOSPIN Cell & Tissue RNA (Nippon Gene, Tokyo, Japan). EU-labeled nascent RNA was biotinylated and captured using a Click-iT® Nascent RNA Capture Kit (Invitrogen) according to manufacturer's instructions.

cDNA synthesis and quantitative PCR

Total RNA (500 ng) or nascent RNA (200 ng) was transcribed using the Verso cDNA Synthesis Kit (Thermo Fisher Scientific). Quantitative PCR was performed on a StepOnePlus Real-Time PCR System (Applied Biosystems, Foster City, CA) with SYBR® Premix Ex *Taq* (TaKaRa) under the following conditions: 95°C for 2 min followed by 40 cycles at 95°C for 3 s and 60°C for 30 s. SGLT2 and HNF1α

8

mRNA levels were normalized to 60S ribosomal protein L13 (RPL13) mRNA levels. The primers used in

this study are listed in Supplemental Table 4.

Nucleosome occupancy and methylome sequencing

Nucleosome occupancy and methylome sequencing (NOMe-Seq) was performed according to

the manufacturer's instructions (Active Motif, Carlsbad, CA) with slight modifications. Approximately 50

mg of frozen human tissues and 7.5×10^5 of HK-2 cells were cross-linked by 1% formaldehyde at room

temperature for 15 and 5 min, respectively, and cross-linking was quenched by adding 1.25 M glycine.

Cells were homogenized in lysis buffer with 40 strokes of a Potter-Elvehjem homogenizer (Wheaton

Industries, Millville, NJ). Homogenized kidney tissues were filtered through an 80-μm Nylon Woven Net

Filter (Merck Millipore, Darmstadt, Germany) to remove tissue debris. Chromatin was sheared to fragments

larger than 1 kb. Sheared chromatin was treated with 0 or 20 U GpC methyltransferase at 37°C for 4 hours.

Reactions were stopped by the addition of stop solution and incubated at 95°C for 15 min. Bisulfite

conversion was then performed on DNA. Bisulfite-converted DNA was used for PCR amplification with

primers for *SGLT2* 5'-FR (Supplemental Table 5). PCR products were cloned into the pGEM®-T easy vector

(Promega). Twenty colonies in GpC methyltransferase-treated DNA and ten colonies in non-treated DNA

were subjected to colony PCR followed by sequencing with primers (Supplemental Table 5) for the

assessment of nucleosome occupancy and CpG methylation, respectively. GpCpG sites were removed from

the analysis of nucleosome occupancy as they are both a GpC and CpG context.

Nucleosome scanning assay

A nucleosome scanning assay (NuSA) was performed using the EpiScope® Nucleosome

Preparation Kit (TaKaRa) according to the manufacturer's protocol with slight modifications.

Approximately 20 mg of the frozen human kidney or 2.0×10^6 of HK-2 cells was washed with ice-cold

phosphate saline buffer and incubated in lysis buffer for 10 min. Tissue samples were homogenized and

filtered as described above. The nuclei released were treated with 0 or 4 U micrococcal nuclease (MNase)

for 30 min at 37°C, and purified using NucleoSpin® Gel and PCR Clean-up (TaKaRa). Nucleosomal DNA

enrichment was evaluated by quantitative PCR with overlapping primer pairs (Supplemental Table 6),

producing a high-resolution, quantitative map of the nucleosome location and occupancy. Relative

nucleosome occupancy was presented by the ratio to the nucleosomal DNA enrichment of LINE-1 as a

reference gene using the Pfaffl method (Pfaffl, 2001).

Chromatin immunoprecipitation assay

Chromatin immunoprecipitation (ChIP) assays were performed using the EpiQuik ChIP or Tissue

ChIP kit (Epigentek, Farmingdale, NY) according to manufacturer's instructions. Briefly, approximately

50 mg of the human kidney or 1.0×10^6 of HK-2 cells were cross-linked, homogenized, and filtered as

described above. Chromatin was sheared to fragments ranging from 300 to 600 bp. The sonicated lysate (5

μL) was used to quantify the total amount of DNA (input). Immunoprecipitation was performed for 90 min

with 2 μg of antibodies: anti-acetylated histone H3 (AcH3; Merck), anti-HNF1α (sc-393925, Santa Cruz

Biotechnology, Santa Cruz, CA), or normal mouse IgG as the negative control. Immunoprecipitated DNA

and input DNA were analyzed by semi-quantitative PCR or quantitative PCR using primers for *SGLT2* 5'-

FR (Supplemental Table 7). Semi-quantitative PCR was performed using Gene RED PCR Mix Plus

(Nippon Gene). PCR products were resolved by electrophoresis on a 2% agarose gel and stained with

ethidium bromide. The intensity of bands was quantified with the Lumino Image Analyzer LAS-3000 and

Multi Gauge (Fujifilm, Tokyo, Japan).

Western blot analysis

The human kidney was pulverized and dissolved in radioimmunoprecipitation assay (RIPA)

buffer (10 mM Tris-HCl pH 7.5, 150 mM NaCl, 1% sodium deoxycholate, 1% NP-40, and 0.1% SDS).

HK-2 cells were harvested and homogenized with RIPA buffer 24 hours after the TSA treatment.

Deglycosylation was performed by incubation with peptide-N-glycosidase F (PNGase F, New England

Biolabs, Ipswich, MA). Lysate samples were separated on 9% SDS-polyacrylamide gels and transferred to

PVDF membranes by Trans-Blot® SD Semi-Dry Electrophoretic Transfer Cell (Bio-Rad, Richmond, CA).

Membranes were blocked in PBS with 0.1% Tween 20 and 5% nonfat dry milk at room temperature for 20

min and incubated with the primary anti-β actin (ab6276, diluted at 1:5000; Abcam, Cambridge, UK), anti-

SGLT2 (sc-393350, diluted at 1:200; Santa Cruz Biotechnology), and anti-HNF1α (sc-6547, diluted at

1:1000; Santa Cruz Biotechnology) antibodies at 4°C overnight. After washing, the membrane was

incubated at room temperature for one hour with the ECL Mouse IgG, HRP-linked whole Ab (NA931,

diluted at 1:10000; GE Healthcare, Little Chalfont, UK) or donkey anti-goat IgG-HRP (sc-2020, diluted at

1:10000; Santa Cruz Biotechnology). After washing the membrane, immune complexes were visualized

11

using a chemiluminescence reagent (Amersham ECL Select; GE Healthcare) and captured with the Lumino

Image Analyzer LAS-3000.

Statistical analysis

Results from three independent experiments are expressed as the mean ± SD. Statistical analyses

were performed with the statistical software program R (R Development Core Team, 2011). The means of

two groups were compared with an unpaired Student's *t*-test (two-tailed). Comparisons of the means of

multiple groups were performed with the Tukey–Kramer test. Two-way analysis of variance (ANOVA) was

used to examine the effects of two factors on an experimental response. All tests were considered significant

at $P < 0.05$.

Results

Analysis of SGLT2 mRNA levels and nucleosome occupancy in HK-2 cells and human kidney tissue

SGLT2 is primarily expressed in the cortex of the kidney and located in the S1 and S2 segments

of the proximal tubule. The HK-2 cell line, an immortalized PTEC line from a normal adult human kidney,

is available as a human PTEC model (Ryan *et al.*, 1994; Wilmer *et al.*, 2010). However, a luciferase assay

with HK-2 cells showed no significant changes in the luciferase activity of *SGLT2* 5'-FR reporter constructs

(Fig. 1A). Quantitative PCR with cDNA synthesized from total RNA and western blot analyses

demonstrated that SGLT2 mRNA and protein levels were markedly lower in HK-2 cells than in the human

kidney (Fig. 1, B and C). These results suggest different regulatory mechanisms for *SGLT2* gene expression

between HK-2 cells and the human kidney. Therefore, we performed nucleosome occupancy and

methylome sequencing (NOMe-Seq) to identify endogenous DNA methylation and the distribution of

nucleosome occupancy in 5'-FR in HK-2 cells and the human kidney. NOMe-Seq results of CpG

methylation profiles showed that 5'-FR was highly methylated in HK-2 and the human kidney (Fig. 2A).

In NOMe-Seq, GpC methyltransferase may artificially methylate GpC sites that are not protected by

nucleosomes or DNA-binding proteins. GpC methylation patterns represent the sites of a genome occupied

by nucleosomes. In order to confirm whether GpC sites in GpC methyltransferase-treated samples were

successfully methylated, we assessed GpC sites in the *GAPDH* promoter. These GpC sites were highly

methylated in extracted DNA samples (Supplemental Fig. 1). 5'-FR was occupied by more nucleosomes in

HK-2 cells than in the human kidney (Fig. 2B and Supplemental Fig. 2A). We then performed NuSA to

confirm nucleosome occupancy in *SGLT2* 5'-FR. Relative nucleosome occupancy was markedly higher in

HK-2 cells than in the human kidney (Fig. 2C). These results indicated that *SGLT2* 5'-FR in HK-2 cells is

highly occupied by nucleosomes.

Influence of the TSA treatment on *SGLT2* expression and nucleosome occupancy in *SGLT2* 5'-FR in

HK-2 cells

Histone acetylation is a well-known mechanism for epigenetic regulation that up-regulates gene

expression. Histone deacetylase inhibitors stimulate gene expression by enhancing histone acetylation. In

the present study, HK-2 cells were treated with TSA, the most common histone deacetylase inhibitor, to

evaluate the effects of histone acetylation on *SGLT2* expression and nucleosome occupancy in *SGLT2* 5'-

MOL#111807

FR. Quantitative PCR with cDNA synthesized from total RNAs showed that the TSA treatment

significantly up-regulated SGLT2 mRNA expression (Fig. 3A). The ChIP assay showed that the TSA

treatment induced the acetylation of histone H3 in the region between -145 to +135 bp upstream of the

SGLT2 transcription start site (TSS), whereas histone H3 acetylation between -547 to -212 bp upstream of

the TSS was not significantly induced (Fig. 3, B, C, and D). We then performed NOMe-Seq and NuSA to

assess changes in nucleosome occupancy in 5'-FR. The nucleosome occupancy level within approximately

300 bp upstream of the TSS was decreased by the TSA treatment, whereas nucleosome occupancy was not

changed in the region between -500 to -300 bp upstream of the TSS (Fig. 4 and Supplemental Fig. 2B).

NOMe-Seq results also showed that the TSA treatment had no effect on endogenous DNA methylation in

5'-FR (Supplemental Fig. 3). These results indicate that histone acetylation by the TSA treatment up-

regulates *SGLT2* expression and decreases nucleosome occupancy levels within approximately 300 bp

upstream of the TSS.

Analysis of HNF1α expression and HNF1α binding frequency after the TSA treatment in HK-2 cells

Transcription factors capable of binding to *SGLT2* 5'-FR were screened by the Database Center

for Life Science Galaxy (Institute in Research Organization of Information and Systems, Japan). A binding

site of HNF1α, which is a transcriptional modulator of *SGLT2* in the human kidney, was found between -

51 to -37 bp (-51/-37) upstream of the *SGLT2* TSS. Chromatin immunoprecipitated (ChIP) assays with

quantitative PCR demonstrated that HNF1α binding was detected in the region between -144 to +26 bp

upstream, including the predicted HNF1α binding site (-51/-37), in the human kidney (Fig. 5A). TSA-

treated HK-2 cells showed a significantly higher binding frequency than DMSO-treated cells (Fig. 5A). We

next performed RNA interference with siHNF1α to evaluate a role for HNF1α in regulating *SGLT2* gene

expression in HK-2 cells. Quantitative PCR and western blot analyses showed that the TSA treatment

caused the up-regulated HNF1α mRNA (Supplemental Fig. 4) and protein expression (Fig. 5, B and C).

The transfection of siHNF1α in DMSO or TSA-treated HK-2 cells significantly decreased HNF1α mRNA

(Supplemental Fig. 4) and protein expression (Fig. 5, B and C). The knockdown of HNF1α decreased

SGLT2 mRNA expression in TSA-treated HK-2 cells, whereas no significant changes were observed in

DMSO-treated HK-2 cells (Fig. 5D). These results suggest that the TSA treatment up-regulates *SGLT2* gene

expression by increased HNF1α binding in *SGLT2* 5'-FR in HK-2 cells.

Deletion analysis of *SGLT2* 5'-FR in HNF1α-expressing HK-2 cells

We performed luciferase assays using HNF1α-expressing HK-2 cells in order to clarify whether

the predicted HNF1α-binding site contributes to the transcription of the *SGLT2* gene (Fig. 6). The

transfection of the HNF1α-negative plasmid (pcDNA3.1) showed that luciferase activity levels were not

significantly different in the four reporter constructs containing *SGLT2* 5'-FR from the control reporter

plasmid (pGL4.10). The transfection of the HNF1α expression plasmid significantly enhanced the

luciferase activities of the -154/+18 construct and -485/+18 construct, whereas no significant differences

were observed in luciferase activities between -154/+18 and -485/+18. These constructs contained the

predicted HNF1α-binding site (-51/-37). We then measured the luciferase activity of the HNF1α-binding

site-deleted construct [del-(-51/-37)]. Cells transfected with del-(-51/-37) demonstrated that the deletion of

MOL#111807

the binding site resulted in loss of HNF1α-mediated luciferase activity. These results suggest that the

predicted HNF1α-binding site (-51/-37) is essential for HNF1α-mediated transcription of the *SGLT2* gene.

Quantitative analysis of effects of the TSA treatment on SGLT2 mRNA levels in HNF1α-expressing HK-2 cells

Quantitative PCR with cDNA synthesized from total RNA and nascent RNA was performed to

evaluate the effects of the TSA treatment on SGLT2 mRNA expression in HNF1α-expressing HK-2 cells

(Fig. 7). In the present study, the nascent RNA was defined as RNA transcribed after the DMSO or TSA

treatment. Total and nascent SGLT2 mRNA expression levels were significantly higher in HNF1α-

expressing cells treated with TSA than in pcDNA3.1-transfected cells. Nascent SGLT2 mRNA levels were

1.8-fold higher than total SGLT2 mRNA in HNF1α-expressing cells treated with TSA. On the other hand,

no significant changes in SGLT2 mRNA expression levels were observed in HNF1α-expressing cells

treated with DMSO. These results indicate that histone acetylation induced by the TSA treatment plays an

important role in the HNF1α-mediated up-regulation of the *SGLT2* gene.

Analysis of nucleosome occupancy in human kidney, liver, and small intestine tissues

HNF1α is expressed in various tissues such as the liver and intestines, whereas *SGLT2* is not. We

attempted to identify nucleosome occupancy in 5'-FR containing the HNF1α-binding site in the human

liver and small intestine. The region within approximately 300 bp upstream of the *SGLT2* TSS showed

markedly higher nucleosome occupancy in the liver and small intestine than in the kidney (Fig. 8). These

results suggest that tissue-specific nucleosome occupancy in 5'-FR plays an important role in the regulation

of *SGLT2* expression via HNF1α binding.

Discussion

In the present study, we focused on the transcriptional regulatory mechanisms of the *SGLT2* gene

in the human kidney. *SGLT2* is known to be expressed in PTECs of the human kidney. Some PTEC lines,

such as LLC-PK1, KPT2, and MDCK cells, have been used to analyze expression and regulation of the

SGLT2 gene in the kidney (Da Costa-Pessoa *et al.*, 2014; Jiang *et al.*, 2014; Zapata-Morales *et al.*, 2014).

The human kidney-derived HK-2 cell line, which is available as a human PTEC model (Ryan *et al.*, 1994;

Wilmer *et al.*, 2010), has been used to evaluate the regulatory mechanism for the *SGLT2* gene in PTECs of

the human kidney (Panchapakesan *et al.*, 2013). The principal portion of the kidney was divided into two

distinct regions: renal cortex and renal medulla. The expression level was extremely higher in renal cortex

than the renal medulla (You *et al.*, 1995; Chen *et al.*, 2010). The proximal tubule, which contains PTECs,

is a portion of the renal cortex. Therefore, we performed *in vitro* analyses using the HK-2 cells derived from

PTECs and the renal cortex to reveal the transcriptional profiles of the *SGLT2* gene in the human kidney.

The regulatory mechanisms for *SGLT2* gene expression in the human kidney remain unclear.

Our results showed that HK-2 cells exhibited weak transcriptional activity for the *SGLT2* gene (Fig. 1A).

We demonstrated that the levels of SGLT2 mRNA and protein expression were extremely lower in HK-2

cells than the human kidney (Fig. 1, B and C). These results suggest that *SGLT2* expression is not activated

in HK-2 cells, which is derived from the PTEC of the human kidney. DNA methylation, which is a well-

known epigenetic mechanism for transcriptional silencing (Jones and Baylin, 2007), plays an important

role in the regulation of tissue-specific gene expression by inhibiting the binding of transcription factors to

DNA (Song *et al.*, 2005; Moore *et al.*, 2013; Medvedeva *et al.*, 2014). Previous studies have reported that

kidney-specific expression of various genes is associated with DNA methylation of the promoter region

around the TSS (Aoki *et al.*, 2008; Kikuchi *et al.*, 2010; Azuma *et al.*, 2012). Our results of the assessment

of CpG methylation using NOMe-Seq demonstrated that all CpG sites in *SGLT2* 5'-FR were highly

methylated in HK-2 cells and the human kidney (Fig. 2A), suggesting that endogenous DNA methylation

is not involved in the regulation of *SGLT2* expression. In contrast, we found that 5'-FR in HK-2 cells was

occupied by more nucleosomes than in the human kidney (Fig. 2B). The highly occupied 5'-FR in HK-2

cells was confirmed by NuSA (Fig. 2C). Nucleosome occupancy may regulate transcription by inhibiting

the access of transcription factors to promoters (Lorch *et al.*, 1987; Kornberg and Lorch, 1999). These

results suggest that the weak *SGLT2* transcriptional activity of HK-2 cells is due to high nucleosome

occupancy in *SGLT2* 5'-FR.

Our results showed that the TSA treatment up-regulated SGLT2 mRNA expression, induced the

acetylation of histone H3, and decreased nucleosome occupancy in 5'-FR within approximately 300 bp

upstream of the *SGLT2* TSS (Figs. 3 and 4). TSA strongly increases the acetylation of the N-terminal tails

of histone H3, which is a well-established acetylation target in nucleosome dynamics and gene activation

(Choi and Howe, 2009; Hansen *et al.*, 2010). Previous studies reported higher levels of histone H3

acetylation and lower nucleosome occupancy at active genes in promoter regions (Strenkert *et al.*, 2011).

Histone acetylation alters the nucleosomal conformation, which may increase the accessibility of

transcriptional factors (Norton *et al.*, 1989; Lee *et al.*, 1993). Most transcribed genes have low nucleosome

occupancy at promoters (Bell *et al.*, 2011). These findings suggest that decreased nucleosome occupancy

in *SGLT2* 5'-FR altered by the TSA-induced acetylation of histone H3 is involved in the up-regulation of

SGLT2 expression via the binding of transcription factors to 5'-FR.

Previous studies demonstrated that the TSA-mediated up-regulation of gene expression is

associated with histone H3 acetylation and the recruitment of HNF1α to the promoter (Yang *et al.*, 2010).

Our results using TSA-treated HK-2 cells showed an enhanced HNF1α binding frequency in *SGLT2* 5'-FR

(Fig. 5A). The knockdown of HNF1α decreased HNF1α protein levels in DMSO- or TSA-treated HK-2

cells (Fig. 5, B and C), but SGLT2 mRNA expression level was significantly decreased in TSA-treated cells

not in DMSO-treated cells (Fig. 5D). Furthermore, the HNF1α overexpression, which was confirmed by

western blot analysis (Supplemental Fig. 5), significantly enhanced the transcriptional activity of 5'-FR

(Fig. 6). These results suggest that the up-regulation of SGLT2 mRNA expression after the TSA treatment

is associated with the enhanced HNF1α binding frequency in 5'-FR. On the other hand, the loss of HNF1α-

mediated transcriptional activity was caused by the deletion of the predicted HNF1α-binding site (Fig. 6).

Previous studies reported that a promoter region of the rodent *Sglt2* gene is located in 5'-FR around the

HNF1α-binding site (Pontoglio *et al.*, 2000; Freitas *et al.*, 2008). In addition, reduction in the HNF1α

binding frequency at the binding site suppresses SGLT2 mRNA expression (Zhao *et al.*, 2016). Collectively,

our results suggest that 5'-FR around the HNF1α-binding site is a promoter region of the *SGLT2* gene.

The up-regulation of SGLT2 mRNA expression by HNF1α was observed in TSA-treated HK-2

cells (Fig. 7). The TSA treatment also caused a decrease in nucleosome occupancy in 5'-FR containing the

HNF1α-binding site (Fig. 4). Histone acetylation decreases nucleosome occupancy and enhances the accessibility of transcription factors to promoter regions (Li *et al.*, 2005; Zampetaki *et al.*, 2007; Haberland *et al.*, 2009). These results indicate that nucleosome occupancy in 5'-FR plays a critical role in interfering with the binding of HNF1α, thereby regulating *SGLT2* expression.

Previous studies reported that *SGLT2* is predominantly expressed in the human kidney (Chen *et al.*, 2010; Wright *et al.*, 2011), whereas HNF1α is strongly expressed in the human kidney, liver, and small intestine (Cereghini, 1996; Harries *et al.*, 2009; D'Angelo *et al.*, 2010). Our results revealed markedly higher nucleosome occupancy in the human liver and small intestine than in the kidney (Fig. 8). In contrast, the results of the assessment of CpG methylation demonstrated that all CpG sites in *SGLT2* 5'-FR were highly methylated in the human kidney, liver, and small intestine (Fig. 2A and Supplemental Fig. 3B). These results suggest that the different nucleosome occupancy levels in these tissues may affect tissue-specific HNF1α binding frequency, and, thus, lead to tissue-specific *SGLT2* expression. This hypothesis is supported by previous findings demonstrating that tissue-specific gene expression is associated with tissue-specific nucleosome occupancy in the upstream region of the TSS (Kikuchi *et al.*, 2010; Chen *et al.*, 2017).

The inhibition of SGLT2 has been reported as a new therapeutic strategy for diabetes (Chao and Henry, 2010; Terami *et al.*, 2014). Previous studies demonstrated that *SGLT2* expression levels are increased in patients with type 2 diabetes (Rahmoune *et al.*, 2005; Wang *et al.*, 2017). On the other hand, the recent study reported that SGLT2 expression was significantly higher in healthy controls than participants with type 2 diabetes (Solini *et al.*, 2017). Decreased *SGLT2* expression levels were observed in patients with maturity onset diabetes of the young type 3 (Pontoglio *et al.*, 2000), caused by mutations

in the *HNF1α* gene (Menzel *et al.*, 1998). However, the mechanisms responsible for the regulation of *SGLT2*

expression in these diabetic patients remain unclear. Our results demonstrated that *SGLT2* expression levels

are associated with the HNF1α binding frequency in 5'-FR. An increased HNF1α binding frequency in the

Sglt2 promoter region is involved in the diabetes-induced overexpression of *Sglt2* in the rat kidney (Freitas

et al., 2008). In addition, a high sodium intake suppresses *SGLT2* expression by reducing the HNF1α

binding frequency in 5'-FR (Zhao *et al.*, 2016). Therefore, a clearer understanding of the HNF1α binding

frequency in 5'-FR in the human kidney will provide new insights into how *SGLT2* expression is regulated

in diabetic patients.

In conclusion, our results clearly demonstrate that the transcriptional regulatory mechanisms for

the *SGLT2* gene are controlled by nucleosome occupancy and HNF1α binding in the *SGLT2* promoter. This

is the first study on epigenetic mechanisms to regulate *SGLT2* expression in human tissues. Further studies

are required in order to investigate in more detail the histone modifications causing alterations in

nucleosome occupancy in the *SGLT2* gene related to the regulation of *SGLT2* expression.

MOL#111807

Authorship Contributions

Participated in research design: Takesue, Hirota, and Ieiri.

Conducted experiments: Takesue, Hirota, Tachimura, and Tokashiki.

Performed data analysis: Takesue and Hirota.

Wrote or contributed to the writing of the manuscript: Takesue, Hirota, and Ieiri.

References

Aoki M, Terada T, Kajiwara M, Ogasawara K, Ikai I, Ogawa O, Katsura T, and Inui K (2008) Kidney-specific expression of human organic cation transporter 2 (OCT2/SLC22A2) is regulated by DNA methylation. *Am J Physiol Renal Physiol* **295**:F165–F170, American Physiological Society.

Azuma M, Koyama D, Kikuchi J, Yoshizawa H, Thasinas D, Shiizaki K, Kuro-O M, Furukawa Y, and Kusano E (2012) Promoter methylation confers kidney-specific expression of the Klotho gene. *FASEB J* **26**:4264–4274, The Federation of American Societies for Experimental Biology.

Bell O, Tiwari VK, Thomä NH, and Schübeler D (2011) Determinants and dynamics of genome accessibility. *Nat Rev Genet* **12**:554–64.

Boldys A, and Okopien B (2009) Inhibitors of type 2 sodium glucose co-transporters - A new strategy for diabetes treatment. *Pharmacol Reports* **61**:778–784.

Bonner C, Kerr-Conte J, Gmyr V, Queniat G, Moerman E, Thévenet J, Beaucamps C, Delalleau N, Popescu I, Malaisse WJ, Sener A, Deprez B, Abderrahmani A, Staels B, and Pattou F (2015) Inhibition of the glucose transporter SGLT2 with dapagliflozin in pancreatic alpha cells triggers glucagon secretion. *Nat Med* **21**:512–7.

Cereghini S (1996) Liver-enriched transcription factors and hepatocyte differentiation. *FASEB J* **10**:267–282.

Chao EC, and Henry RR (2010) SGLT2 inhibition--a novel strategy for diabetes treatment. *Nat Rev Drug Discov* **9**:551–559, Nature Publishing Group.

Chen J, Li E, Zhang X, Dong X, Lei L, Song W, Zhao H, and Lai J (2017) Genome-wide nucleosome

occupancy and organization modulates the plasticity of gene transcriptional status in maize. *Mol Plant* **10**:962–974.

Chen J, Williams S, Ho S, Loraine H, Hagan D, Whaley JM, and Feder JN (2010) Quantitative PCR tissue expression profiling of the human SGLT2 gene and related family members. *Diabetes Ther* **1**:57–92.

Choi JK, and Howe LJ (2009) Histone acetylation: truth of consequences? *Biochem Cell Biol* **87**:139–150.

D'Angelo A, Bluteau O, Garcia-Gonzalez MA, Gresh L, Doyen A, Garbay S, Robine S, and Pontoglio M (2010) Hepatocyte nuclear factor 1alpha and beta control terminal differentiation and cell fate commitment in the gut epithelium. *Development* **137**:1573–1582.

Da Costa-Pessoa JM, Damasceno RS, Machado UF, Beloto-Silva O, and Oliveira-Souza M (2014) High glucose concentration stimulates NHE-1 activity in distal nephron cells: The role of the Mek/Erk1/2/p90 and p38MAPK signaling pathways. *Cell Physiol Biochem* **33**:333–343, Karger Publishers.

Freitas HS, Anhê GF, Melo KFS, Okamoto MM, Oliveira-Souza M, Bordin S, and Machado UF (2008) Na^+-glucose transporter-2 messenger ribonucleic acid expression in kidney of diabetic rats correlates with glycemic levels: Involvement of hepatocyte nuclear factor-1α expression and activity. *Endocrinology* **149**:717–724.

Gerich JE (2010) Role of the kidney in normal glucose homeostasis and in the hyperglycaemia of diabetes mellitus: Therapeutic implications. *Diabet Med* **27**:136–142.

Haberland M, Montgomery RL, and Olson EN (2009) The many roles of histone deacetylases in

development and physiology: implications for disease and therapy. *Nat Rev Genet* **10**:32–42.

Hansen JC, Nyborg JK, Luger K, and Stargell LA (2010) Histone chaperones, histone acetylation, and the

fluidity of the chromogenome. *J Cell Physiol* **224**:289–99, NIH Public Access.

Harries LW, Brown JE, and Gloyn AL (2009) Species-specific differences in the expression of the

HNF1A, HNF1B and HNF4A genes. *PLoS One* **4**:e7855, Public Library of Science.

Hoffman BG, Robertson G, Zavaglia B, Beach M, Cullum R, Lee S, Soukhatcheva G, Li L, Wederell ED,

Thiessen N, Bilenky M, Cezard T, Tam A, Kamoh B, Birol I, Dai D, Zhao Y, Hirst M, Verchere

CB, Helgason CD, Marra MA, Jones SJM, and Hoodless PA (2010) Locus co-occupancy,

nucleosome positioning, and H3K4me1 regulate the functionality of FOXA2-, HNF4A-, and

PDX1-bound loci in islets and liver. *Genome Res* **20**:1037–1051, Cold Spring Harbor Laboratory

Press.

Hu G, Schones DE, Cui K, Ybarra R, Northrup D, Tang Q, Gattinoni L, Restifo NP, Huang S, and Zhao

K (2011) Regulation of nucleosome landscape and transcription factor targeting at tissue-specific

enhancers by BRG1. *Genome Res* **21**:1650–1658, Cold Spring Harbor Laboratory Press.

Jabbour S, and Goldstein B (2008) Sodium glucose co transporter 2 inhibitors: blocking renal tubular

reabsorption of glucose to improve glycaemic control in patients with diabetes. *Int J Clin Pract*

62:1279–1284.

Jiang M, Wang Q, Karasawa T, Koo JW, Li H, and Steyger PS (2014) Sodium-glucose transporter-2

(SGLT2; SLC5A2) enhances cellular uptake of aminoglycosides. *PLoS One* **9**:e108941, Public

Library of Science.

Jones PA, and Baylin SB (2007) The Epigenomics of Cancer. *Cell* **128**:683–692.

Kikuchi R, Yagi S, Kusuhara H, Imai S, Sugiyama Y, and Shiota K (2010) Genome-wide analysis of

epigenetic signatures for kidney-specific transporters. *Kidney Int* **78**:569–577, Elsevier.

Kornberg RD, and Lorch Y (1999) Twenty-five years of the nucleosome, fundamental particle of the

eukaryote chromosome. *Cell* **98**:285–294.

Kothinti RK, Blodgett AB, Petering DH, and Tabatabai NM (2010) Cadmium down-regulation of kidney

Sp1 binding to mouse SGLT1 and SGLT2 gene promoters: Possible reaction of cadmium with the

zinc finger domain of Sp1. *Toxicol Appl Pharmacol* **244**:254–262.

Lee DY, Hayes JJ, Pruss D, and Wolffe AP (1993) A positive role for histone acetylation in transcription

factor access to nucleosomal DNA. *Cell* **72**:73–84.

Li B, Pattenden SG, Lee D, Gutiérrez J, Chen J, Seidel C, Gerton J, and Workman JL (2005) Preferential

occupancy of histone variant H2AZ at inactive promoters influences local histone modifications

and chromatin remodeling. *Proc Natl Acad Sci U S A* **102**:18385–18390.

López GP, Albarrán OG, and Megías MC (2010) Sodium-glucose cotransporter 2 (SGLT2) inhibitors:

from renal glycosuria to the treatment of type 2 diabetes mellitus. *Nefrologia* **30**:618–625.

Lorch Y, LaPointe JW, and Kornberg RD (1987) Nucleosomes inhibit the initiation of transcription but

allow chain elongation with the displacement of histones. *Cell* **49**:203–210.

Medvedeva YA, Khamis AM, Kulakovskiy I V, Ba-Alawi W, Bhuyan MSI, Kawaji H, Lassmann T,

Harbers M, Forrest ARR, and Bajic VB (2014) Effects of cytosine methylation on transcription

factor binding sites. *BMC Genomics* **15**:119, BioMed Central.

Menzel R, Kaisaki PJ, Rjasanowski I, Heinke P, Kerner W, and Menzel S (1998) A low renal threshold for glucose in diabetic patients with a mutation in the hepatocyte nuclear factor-1α (HNF-1α) gene. *Diabet Med* **15**:816–820, John Wiley & Sons, Ltd.

Misra M (2013) SGLT2 inhibitors: a promising new therapeutic option for treatment of type 2 diabetes mellitus. *J Pharm Pharmacol* **65**:317–27.

Moore LD, Le T, and Fan G (2013) DNA methylation and its basic function. *Neuropsychopharmacology* **38**:23–38, Nature Publishing Group.

Nishimura K, Ide R, Hirota T, Kawazu K, Kodama S, Takesue H, and Ieiri I (2014) Identification and functional characterization of novel nonsynonymous variants in the human multidrug and toxin extrusion 2-K. *Drug Metab Dispos* **42**:1432–1437.

Norton VG, Imai BS, Yau P, and Bradbury EM (1989) Histone acetylation reduces nucleosome core particle linking number change. *Cell* **57**:449–457.

Panchapakesan U, Pegg K, Gross S, Komala MG, Mudaliar H, Forbes J, Pollock C, and Mather A (2013) Effects of SGLT2 Inhibition in Human Kidney Proximal Tubular Cells-Renoprotection in Diabetic Nephropathy? *PLoS One* **8**:e54442.

Pfaffl M (2001) A new mathematical model for relative quantification in real-time RT–PCR. *Nucleic Acids Res* **29**:16–21.

Pontoglio M, Prié D, Cheret C, Doyen A, Leroy C, Froguel P, Velho G, Yaniv M, and Friedlander G (2000) HNF1alpha controls renal glucose reabsorption in mouse and man. *EMBO Rep* **1**:359–65.

Rahmoune H, Thompson PW, Ward JM, Smith CD, Hong G, and Brown J (2005) Glucose transporters in human renal proximal tubular cells isolated from the urine of patients with non-insulin-dependent diabetes. *Diabetes* **54**:3427–3434.

Ryan MJ, Johnson G, Kirk J, Fuerstenberg SM, Zager RA, and Torok-Storb B (1994) HK-2: an immortalized proximal tubule epithelial cell line from normal adult human kidney. *Kidney Int* **45**:48–57.

Solini A, Rossi C, Mazzanti CM, Proietti A, Koepsell H, and Ferrannini E (2017) SGLT2 and SGLT1 renal expression in patients with type 2 diabetes. *Diabetes, Obes Metab* **19**:1289–1294.

Song F, Smith JF, Kimura MT, Morrow AD, Matsuyama T, Nagase H, and Held WA (2005) Association of tissue-specific differentially methylated regions (TDMs) with differential gene expression. *Proc Natl Acad Sci U S A* **102**:3336–41, National Academy of Sciences.

Strenkert D, Schmollinger S, Sommer F, Schulz-Raffelt M, and Schroda M (2011) Transcription factor-dependent chromatin remodeling at heat shock and copper-responsive promoters in Chlamydomonas reinhardtii. *Plant Cell* **23**:2285–301.

Terami N, Ogawa D, Tachibana H, Hatanaka T, Wada J, Nakatsuka A, Eguchi J, Sato Horiguchi C, Nishii N, Yamada H, Takei K, and Makino H (2014) Long-term treatment with the sodium glucose cotransporter 2 inhibitor, dapagliflozin, ameliorates glucose homeostasis and diabetic nephropathy in db/db mice. *PLoS One* **9**:e100777, Public Library of Science.

Tsui K, Dubuis S, Gebbia M, Morse RH, Barkai N, Tirosh I, and Nislow C (2011) Evolution of Nucleosome Occupancy: Conservation of Global Properties and Divergence of Gene-Specific

Patterns. *Mol Cell Biol* **31**:4348–4355, American Society for Microbiology (ASM).

Vallon V, Rose M, Gerasimova M, Satriano J, Platt KA, Koepsell H, Cunard R, Sharma K, Thomson SC, and Rieg T (2013) Knockout of Na-glucose transporter SGLT2 attenuates hyperglycemia and glomerular hyperfiltration but not kidney growth or injury in diabetes mellitus. *Am J Physiol Ren Physiol* **304**:F156–F167.

Wang XX, Levi J, Luo Y, Myakala K, Herman-Edelstein M, Qiu L, Wang D, Peng Y, Grenz A, Lucia S, Dobrinskikh E, D'Agati VD, Koepsell H, Kopp JB, Rosenberg AZ, and Levi M (2017) SGLT2 protein expression is increased in human diabetic nephropathy: SGLT2 protein inhibition decreases renal lipid accumulation, inflammation, and the development of nephropathy in diabetic mice. *J Biol Chem* **292**:5335–5348.

Wilmer MJ, Saleem MA, Masereeuw R, Ni L, Van Der Velden TJ, Russel FG, Mathieson PW, Monnens LA, Van Den Heuvel LP, and Levtchenko EN (2010) Novel conditionally immortalized human proximal tubule cell line expressing functional influx and efflux transporters. *Cell Tissue Res* **339**:449–457.

Workman JL (2006) Nucleosome displacement in transcription. *Genes Dev* **20**:2009–2017.

Wright EM (2001) Renal Na $^+$ -glucose cotransporters. *Am J Physiol Physiol* **280**:F10–F18.

Wright EM, Loo DDF, and Hirayama BA (2011) Biology of human sodium glucose transporters. *Physiol Rev* **91**:733–794.

Yang H, Nie Y, Li Y, and Wan Y-JY (2010) Histone modification-mediated CYP2E1 gene expression and apoptosis of HepG2 cells. *Exp Biol Med (Maywood)* **235**:32–39, NIH Public Access.

Yang Z, Yoshioka H, and McCarrey JR (2013) Sequence-specific promoter elements regulate temporal-specific changes in chromatin required for testis-specific activation of the Pgk2 gene. *Reproduction* **146**:501–516, Society for Reproduction and Fertility.

You G, Lee WS, Barros EJG, Kanai Y, Huo TL, Khawaja S, Wells RG, Nigam SK, and Hediger MA (1995) Molecular characteristics of Na+-coupled glucose transporters in adult and embryonic rat kidney. *J Biol Chem* **270**:29365–29371, American Society for Biochemistry and Molecular Biology.

Zampetaki A, Zeng L, Xiao Q, Margariti A, Hu Y, and Xu Q (2007) Lacking cytokine production in ES cells and ES-cell-derived vascular cells stimulated by TNF-alpha is rescued by HDAC inhibitor trichostatin A. *Am J Physiol Cell Physiol* **293**:C1226-38.

Zapata-Morales JR, Galicia-Cruz OG, Franco M, and Morales FM (2014) Hypoxia-inducible factor-1α(HIF-1α) protein diminishes sodium glucose transport 1 (SGLT1) and SGLT2 protein expression In renal epithelial tubular cells (LLC-PK1) under hypoxia. *J Biol Chem* **289**:346–357.

Zhang T, Zhang W, and Jiang J (2015) Genome-Wide Nucleosome Occupancy and Positioning and Their Impact on Gene Expression and Evolution in Plants. *Plant Physiol* **168**:1406–1416, American Society of Plant Biologists.

Zhao Y, Gao P, Sun F, Li Q, Chen J, Yu H, Li L, Wei X, He H, Lu Z, Wei X, Wang B, Cui Y, Xiong S, Shang Q, Xu A, Huang Y, Liu D, and Zhu Z (2016) Sodium Intake Regulates Glucose Homeostasis through the PPARδ/Adiponectin-Mediated SGLT2 Pathway. *Cell Metab* **23**:699–711.

MOL#111807

Footnotes

MOL#111807

Figure Legends

Fig. 1. Analysis of transcriptional activity of *SGLT2* 5'-FR and SGLT2 expression levels in HK-2 cells

(A) Luciferase activity of a series of reporter constructs containing *SGLT2* 5'-FR in HK-2 cells. Results are expressed as fold increases in pGL4.10. (B) SGLT2 mRNA levels in HK-2 cells and the human kidney were measured by quantitative PCR and normalized to RPL13 mRNA levels. Results are expressed relative to SGLT2 mRNA levels in the human kidney. (C) Western blot analyses of SGLT2 and β-actin protein expression in HK-2 cells and the human kidney. SGLT2 protein levels represent the density ratio for the bands of SGLT2 and β-actin. Results are expressed relative to SGLT2 protein levels in the human kidney. Results represent the mean ± SD of three independent experiments. $*P < 0.05$.

Fig. 2. Analysis of epigenetic regulation in *SGLT2* 5'-FR in HK-2 cells and the human kidney

(A and B) NOMe-Seq data of *SGLT2* 5'-FR in HK-2 cells and the human kidney. The arrow indicates the *SGLT2* TSS. (A) Vertical lines indicate CpG sites. White circles represent unmethylated CpG sites and black circles represent methylated CpG sites. (B) Vertical lines indicate GpC sites. White circles represent unmethylated GpC sites and black circles represent methylated GpC sites. Deep gray bars represent nucleosome occupancy, which is the region of consecutive unmethylated GpC sites over 147 bp. (C) NuSA data of 5'-FR in HK-2 cells (black circles) and the human kidney (white circles). Relative nucleosome occupancy is expressed relative to the level of nucleosome occupancy in each sample without the MNase treatment and indicated by the midpoints of each amplicon. Results represent the mean ± SD of three

independent experiments. *$P < 0.05$ for HK-2 cells versus the human kidney.

Fig. 3. Influence of the TSA treatment on *SGLT2* expression and histone acetylation in *SGLT2* 5'-FR in HK-2 cells

HK-2 cells were treated with DMSO or TSA for 24 hours. (A) SGLT2 mRNA levels were measured by quantitative PCR and normalized to RPL13 mRNA levels. Results are expressed relative to SGLT2 mRNA levels in DMSO-treated cells (control). (B) Scheme of the ChIP assay in 5'-FR. The upper arrow indicates the *SGLT2* TSS. Lower arrows indicate two sets of PCR primers targeting 5'-FR, designated as distal and proximal. (C) ChIP analyses targeting 5'-FR in DMSO- or TSA-treated cells using antibodies against normal IgG (white bars) and AcH3 (black bars). (D) Semi-quantitative analyses of AcH3 enrichment in two regions in ChIP analyses in (C). Results are expressed as the percentage of the immunoprecipitate over total input DNA. Results represent the mean ± SD of three independent experiments. *$P < 0.05$.

Fig. 4. Influence of the TSA treatment on nucleosome occupancy in *SGLT2* 5'-FR in HK-2 cells

(A) NOMe-Seq data of *SGLT2* 5'-FR in DMSO- or TSA-treated cells. Vertical lines indicate GpC sites. White circles represent unmethylated GpC sites and black circles represent methylated GpC sites. Deep gray bars represent nucleosome occupancy, which is the region of consecutive unmethylated GpC sites over 147 bp. (B) NuSA data of 5'-FR in DMSO- (black circles) or TSA-treated cells (white circles). Relative nucleosome occupancy is expressed relative to the level of nucleosome occupancy in each sample without the MNase treatment and indicated by the midpoints of each amplicon. Results represent the mean ± SD of

three independent experiments. *P* < 0.05 for DMSO group versus TSA group.

Fig. 5. Analysis of HNF1α expression and HNF1α binding frequency after the TSA treatment in HK-2 cells

(A) ChIP analyses with quantitative PCR targeting the HNF1α-binding site in *SGLT2* 5'-FR in DMSO- or TSA-treated cells and the human kidney using antibodies against normal IgG (white bars) and HNF1α (black bars). The relative binding frequency of HNF1α was measured by quantitative PCR and normalized to that of the input. (B) HK-2 cells were reverse-transfected with negative control or siHNF1α for 24 hours, and then treated with DMSO or TSA for 24 hours. Western blot analyses representing HNF1α and β-actin protein expression in HK-2 cells. (C) Protein levels represent the density of the ratio for the bands of HNF1α and β-actin in (B). Results were normalized to HNF1α protein levels in DMSO-treated cells (control). (D) SGLT2 mRNA levels were measured by quantitative PCR and normalized to RPL13 mRNA levels. Results are expressed relative to SGLT2 mRNA levels in DMSO-treated cells. Results represent the mean ± SD of three independent experiments. *P* < 0.05.

Fig. 6. Deletion analysis of *SGLT2* 5'-FR in HNF1α-expressing HK-2 cells

HK-2 cells were transfected with a series of reporter constructs or a control reporter plasmid (pGL4.10), together with the HNF1α-negative plasmid (pcDNA3.1, white bars) or HNF1α expression plasmid (black bars). The position of the deleted region is indicated with 'Del-(-51/-37)'. Relative luciferase activity is expressed as a fold increase in pGL4.10 and represents the mean ± SD of three independent experiments.

P < 0.05.

Fig. 7. Quantitative analysis of effects of the TSA treatment on SGLT2 mRNA levels in HNF1α-expressing HK-2 cells

HK-2 cells were transfected with the HNF1α-negative plasmid (pcDNA3.1, white circles) or HNF1α expression plasmid (black circles) and treated with DMSO or TSA for 24 hours. Total and nascent SGLT2 mRNA levels were measured by quantitative PCR and normalized to RPL13 mRNA levels. Results are expressed relative to SGLT2 mRNA levels in empty pcDNA3.1-transfected cells treated with DMSO. Results represent the mean ± SD of three independent experiments. *P* < 0.05 for HNF1α group versus pcDNA3.1 group.

Fig. 8. Analysis of nucleosome occupancy in human kidney, liver, and small intestine tissues

NOMe-Seq data of *SGLT2* 5'-FR in the human kidney (white squares), liver (white circles), and small intestine (black circles). Graph represents the proportion of nucleosome-occupied GpC sites in 5'-FR in the three tissues. The arrow indicates the *SGLT2* TSS. Vertical lines indicate GpC sites.
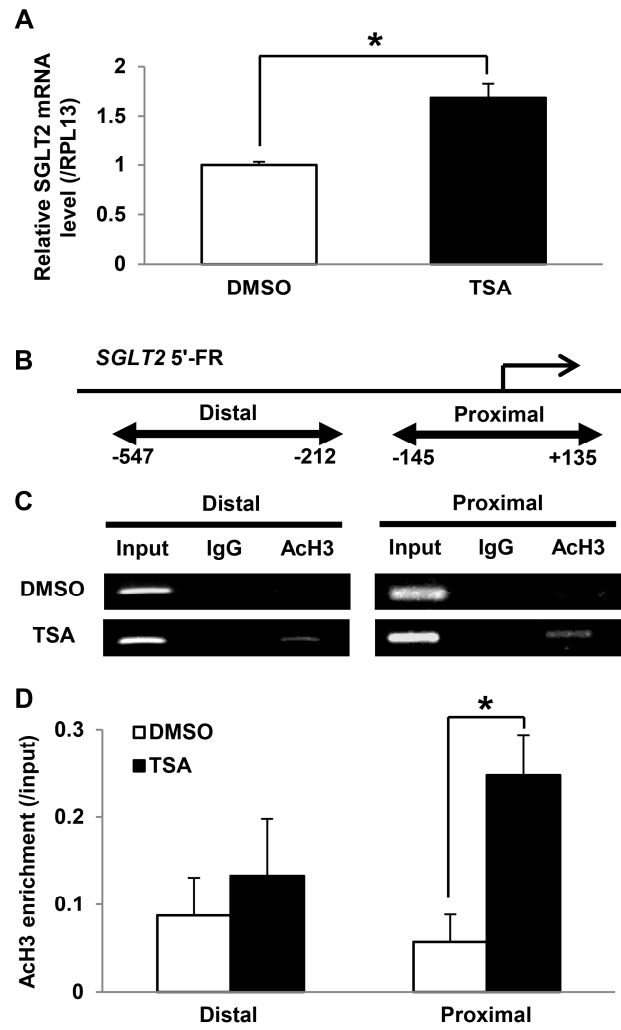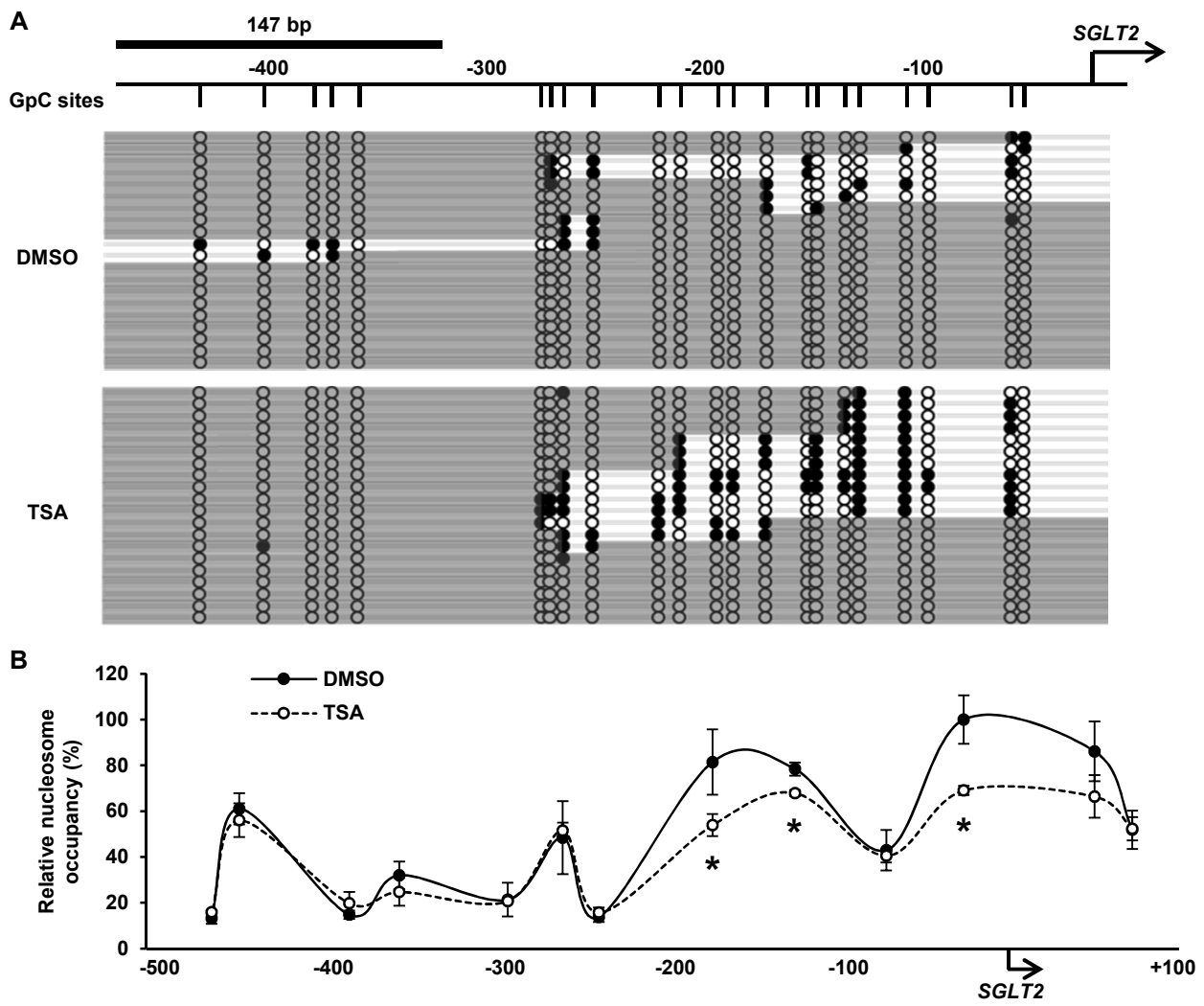
Fig. 1

Fig. 2

Fig. 3

Fig. 4

A

B

C

D

Fig. 5

Fig. 6

Fig. 7

Fig. 8